Zeitschrift für Geophysik, 1970, Band 36, Seite 655–678. Physica-Verlag, Würzburg

Scattering of Low-Frequency Sound in the Ocean

By H.-H. ESSEN and K. HASSELMANN, Hamburg[1])

Eingegangen am 27. April 1970

Summary: The scattering of acoustic modes by inhomogeneities in an oceanic wave guide is investigated in the weak-interaction approximation. Application to the case of interactions with surface gravity waves yields maximal damping factors due to scattering losses in the range $10^{-2}-10^{-3}$, in order-of-magnitude agreement with measurements. The calculations are based on an empirical PIERSON-MOSKOWITZ wave spectrum and a two-layer wave-guide model. The scattered field for a given mode of a point source is computed in the single-scattering approximation. Simultaneous measurements of the primary-signal attenuation, the surface wave spectrum and the Doppler sprectrum of the scattered field would provide independent quantitative comparisons between theory and experiment.

Zusammenfassung: Die Streuung von akustischen Eigenschwingungen durch Inhomogenitäten eines ozeanischen Wellenleiters wird in der Näherung schwacher Wechselwirkungen untersucht. Die Anwendung auf Wechselwirkungen mit Oberflächenschwerewellen liefert maximale Dämpfungsfaktoren durch Streuverluste im Bereich $10^{-2}-10^{-3}$, größenordnungsmäßig übereinstimmend mit Messungen. Die Rechnungen basieren auf einem empirischen PIERSON-MOSKOWITZ-Seegangsspektrum und einem Zwei-Schichten-Modell des Wellenleiters. Das gestreute Feld für eine vorgegebene Eigenschwingung einer Punktquelle wird in der ersten Streunäherung berechnet. Gleichzeitige Messungen der Dämpfung des Primärsignales, des Seegangsspektrums und der Doppler-Verschiebung des gestreuten Feldes würden unabhängige quantitative Vergleiche zwischen Theorie und Experiment erlauben.

1. Introduction

The transmission of sound in the ocean is strongly affected by small-scale inhomogeneities of the wave-guide. For low-frequency waves, the scattering loss due to interactions with inhomogeneities of length scales comparable with the acoustic wavelength greatly exceeds the molecular damping. Since the exponential decay due to scattering also dominates asymptotically over the geometric decay factors, the far-field amplitude of the primary signal is largely determined by the scattering loss. The signal-to-noise ratio is also affected by the incoherent scattered field, which generally contains little signal information and therefore contributes mainly to the background noise. Hence meaningful estimates of the hydroacoustic transmission range and its dependence on environmental conditions require an understanding of the basic scattering processes determining both the primary and scattered fields.

[1]) Professor Dr. KLAUS HASSELMANN, Institut für Geophysik der Universität Hamburg, 2 Hamburg 13, Schlüterstr. 22.

Previous theoretical investigations have concentrated mainly on the scattering of a single incident wave train by random inhomogeneities, usually at a rough surface. A recent summary of this work in relation to hydroacoustic wave propagation has been given by FORTUIN [1969]. The approach is adapted to the ray description of sound propagation, in which the field trapped in the wave guide is represented by rays reflected back and forth between the upper and lower boundaries of the ocean. Ray methods are restricted to high frequency fields, and are useful primarily for the investigation of first arrivals, or the wave field close to source; in general, to applications in which the number of separate ray paths contributing to the field is limited.

However, scattering is important mainly in the converse situation, i.e. large distances from the source, and times significantly later than the first arrival time (or continuous sources). In this case, normal-mode representations are more useful than ray descriptions, and it appears natural to investigate hydroacoustic scattering in terms of continuous mode-mode interactions, rather than single-beam scattering theory.

We consider in this paper the scattering of a given (trapped) acoustic mode by wave-guide inhomogeneities, due either to timedependent variations at the surface and within the fluid (surface and internal gravity waves), or the physical inhomogeneities of the bottom topography and the underlying stratification. The scattering of an arbitrary wave field can be determined from single-mode scattering by superposition.

The interactions lead to a transfer of energy from the primary mode into other trapped modes and into the leaking-mode continuum. In the trapped-trapped interaction, nearly all of the energy lost by the primary mode reappears in a random acoustic wave field of approximately the same frequency, the signal is "randomised". In the trapped-leaking interaction, the energy transferred from the primary wave is radiated into the lower half-space and is lost from the wave-guide. The primary signal decays exponentially, without a corresponding increase in the scattered noise level.

If the set of all *trapped* modes of the wave-guide are regarded as a "physical system", the trapped-trapped interactions represent conservative processes which fall within the general formalism for conservative wave-wave interactions (cf. [HASSELMANN, 1966]). The trapped-leaking interactions are non-conservative with respect to this system, but can be treated by a corresponding generalisation of the theory to include non-symmetrical coupling coefficients [HASSELMANN, 1967, 1968].

Alternatively, all interactions can be regarded as conservative by closing the wave guide with a very deep, totally reflecting bottom below the elastic layer. This transforms the leaking-mode continuum into discrete trapped modes. It can be shown that the interactions between "shallow" and "deep" trapped modes yield the same energy transfer in the limit of an infinitely deep bottom as the nonconservative (parametric) interactions for an unbounded, open system*). We shall make use of this equivalence to give a unified discussion in terms of conservative wave-wave interactions only.

*) This is not immediately obvious on account of the two-timing limit involved in the derivation of the transfer expressions. Formally, the two-timing limit cannot be interchanged with the infinite-depth limit.

However, in computing the transfer expressions it is simpler to consider an unbounded open system from the beginning, rather than go to the infinite-depth limit of a closed system (cf. [ESSEN, 1970]).

Numerical results are presented for the case of scattering by surface gravity waves. For simplicity, the computations were carried out for the model of a homogeneous fluid over a homogeneous solid half-space, but the analysis is applicable also to arbitrary, continuously stratified models, such as a SOFAR wave-guide. A PIERSON-MOSKOWITZ surface-wave spectrum yields maximum damping parameters (inverse e-folding distances in units of wavelength) typically of the order 10^{-2}—10^{-3}.

Although existing field measurements do not permit a detailed quantitative comparison with theory, the theoretical damping factors of the primary signal and the Doppler shifts of the scattered field are in reasonable order-of-magnitude agreement with experiment (cf. [TOLSTOY, 1966, SCRIMGER, 1961, NICHOLS, 1967, URICK, 1968]).

2. The mode-mode scattering formalism

We consider weak nonlinear interactions between the normal modes of a stably stratified fluid over a stratified elastic half-space. The physical system is assumed to be homogeneous in the horizontal plane ($x = x_1, x_2$), except for small physical inhomogeneities of zero mean. Slow variations of the mean wave-guide properties can be allowed for in the usual manner (equation 8), but are not relevant for scattering.

For small displacements, the system can be described to first order by the linearised equations of motions. The general solution consists of a superposition of normal modes (cf. [EWING, JARDETZKY, and PRESS, 1957]). To obtain an energetically closed system, we introduce a totally reflecting bottom of the elastic layer at a large, but finite, depth, going later to the infinite-depth limit. Introducing normal-mode coordinates, the complete nonlinear equations of motion of the closed system can then be written in the form [HASSELMANN, 1966],

$$\left(\frac{\partial}{\partial t} + i\omega_\nu\right) a_\nu = -3\, i\omega_\nu \Sigma\, D_{\bar{\nu}\mu\lambda} a_\mu a_\lambda - 4\, i\omega_\nu \Sigma\, D_{\bar{\nu}\mu\lambda\iota} a_\mu a_\lambda a_\iota - \ldots \tag{1}$$

where a_ν represents the (time dependent) amplitude of a suitably normalised normal mode

$$\varphi_\nu(t, \boldsymbol{x}, x_3) = a_\nu(t)\, \psi_\nu(x_3)\, e^{i\boldsymbol{k}\boldsymbol{x}} \tag{2}$$

and $\psi_\nu(x_3)$ denotes a vertical eigenfunction. The composite index ν includes the discrete mode index n and the continuous wavenumber variable $\boldsymbol{k} = (k_1, k_2)$: $\nu = (n, \boldsymbol{k})$.

The left hand side of equation (1) represents the linearised equations of motion in diagonal form, whereas the right hand side describes the nonlinear coupling between modes. The coupling coefficients $D_{\alpha\beta\gamma}$, $D_{\alpha\beta\gamma\delta}$ ... are symmetrical with respect to their indices on account of energy and momentum conservation.

Without coupling, the linear solutions are given by

$$a_\nu(t) = A_\nu e^{-i\omega_\nu t} \tag{3}$$

where A_ν = constant and ω_ν is the eigenfrequency of the mode ν. The normalisation is chosen such that $a_\nu a_\nu^*$ represents the total energy of the mode ν.

To each normal mode (2) there corresponds a complex conjugate solution with negative eigenfrequency. In linear problems, the complex conjugate mode is not usually regarded as a separate solution, since one is interested only in the real part of the field. However, in nonlinear problems the operation of taking the real part does not commute with multiplication, and real fields have to be constructed by adding the complex conjugate solution. It is convenient to denote the complex conjugate mode to ν by a negative index $-\nu$, or the index $\bar{\nu} = -\nu = (-n, -\boldsymbol{k})$, so that $\omega_\nu = -\omega_{\bar{\nu}} = -\omega_{-\nu}$. For real fields, $a_\nu = a_{\bar{\nu}}^*$. The sign convention is chosen such that positive indices correspond to positive frequencies and the wavenumber $\boldsymbol{k}$ points in the positive propagation direction for both ν and $\bar{\nu}$. The summation in equation (1) extends over positive and negative indices.

The nonlinear coupling gives rise to further, forced wave components, whose frequencies and wavenumbers do not satisfy the dispersion relation for free propagation. At the same time, the free components undergo secular changes due to resonant interactions between sets of three or more free components whose frequency and wavenumber sums vanish. The resonant transfer mechanism was first considered in detail in [PEIERLS, 1929] classic paper on the heat conduction in solids and plays an important role in various scattering problems of theoretical physics. Recently, resonant wave-wave interactions have also gained interest in a number of applications in plasmas, fluid dynamics and geophysics. The general formulae for the resonant energy transfer for nonlinear equations of the form (1) are given, e.g., in [HASSELMANN, 1966].

We consider here the appropriate lowest-order transfer expressions for the particular case that a) the energy E_ν of the primary acoustic wave field is concentrated in a spectral line at the wave number $\boldsymbol{k}_n$ of mode n, and b) the remaining energy in the wave-guide consists of a spectral continuum of trapped gravitational and acoustic modes. The fields are assumed to be locally homogeneous, but the spectra are regarded as slowly varying in space and time. The transport equation for the primaryacoustic wave field then reduces to the form (cf. [HASSELMANN, 1968])

$$\frac{\partial E_\nu}{\partial t} + V(\boldsymbol{V}_\nu E_\nu) = -(\gamma_\nu^{tt} + \gamma_\nu^{tl})\, E_\nu \tag{4}$$

where $\boldsymbol{V}_\nu$ is the group velocity of the mode ν.

The damping coefficient

$$\gamma_\nu^{tt} = \sum_{\substack{l>0 \\ m \gtrless 0}} \int T_{\lambda\nu\mu} \frac{F_\mu}{\omega_\mu} \delta(\omega_\lambda - \omega_\mu - \omega_\nu)\, \mathrm{d}\boldsymbol{k}_m \tag{5}$$

$$\lambda = (l, \boldsymbol{k}_l),\ \mu = (m, \boldsymbol{k}_m)$$

describes the energy loss of the mode ν ($n > 0$) due to trapped-trapped scattering, and

$$\gamma_\nu^{tl} = \sum_{m \gtrless 0} \int T_{\nu\mu} F_\mu\, \mathrm{d}\boldsymbol{k}_m \tag{6}$$

describes the loss due to trapped-leaking scattering in the limit of an infinitely deep wave-guide.

The spectrum $F_\mu = F_m(\boldsymbol{k})$ of the mode μ is defined as $F_m(\boldsymbol{k})\,\Delta\boldsymbol{k} = \Sigma\, \frac{1}{2} \langle a_\mu a_{\bar{\mu}} \rangle$, where $\mu = (m, \boldsymbol{k})$ and the sum is taken over an infinitesimal wavenumber element $\Delta\boldsymbol{k}$. The definition applies to both positive and negative indices, $F_\mu = F_m(\boldsymbol{k}) = F_{-m}(-\boldsymbol{k}) = F_{\bar{\mu}}$, the normalisation being such that $F_\mu + F_{\bar{\mu}} = 2F_\mu$ corresponds to the usual spectrum of mode energy. The factor 2 arises from our use of a two-sided spectrum. The energy E_ν is also defined in the two-sided sense, i.e. $F_\nu = F_n(\boldsymbol{k}) = E_\nu\, \delta(\boldsymbol{k} - \boldsymbol{k}_n)$, $F_{\bar{\nu}} = F_{-n}(-\boldsymbol{k}) = E_{\bar{\nu}}\, \delta(\boldsymbol{k} + \boldsymbol{k}_n)$, so that $E_\nu = E_{\bar{\nu}}$ and the total energy of the primary mode ν is $2E_\nu$. The summations in equation (5), (6) extend again over both positive and negative indices (however, in equation (5) the frequency resonance condition can be satisfied only for $l > 0$, see below).

The transfer function for trapped-trapped scattering is given by

$$T_{\lambda\nu\mu} = 72\pi\, \omega_\lambda \omega_\nu \omega_\mu\, |D_{\lambda\nu\mu}|^2 \qquad \text{with } \boldsymbol{k}_l = \boldsymbol{k}_n + \boldsymbol{k}_m. \tag{7}$$

The transfer function for trapped-leaking scattering is obtained by taking the infinite-depth limit of expression (5),

$$T_{\nu\mu} = \left\{ T_{\lambda\nu\mu} \left[\omega_\mu \frac{\partial\omega_\lambda}{\partial l} \right]^{-1} \right\}_{\substack{\omega_\lambda = \omega_\nu + \omega_\mu \\ \boldsymbol{k}_l = \boldsymbol{k}_n + \boldsymbol{k}_m}} \tag{8}$$

where the index l refers to a leaking mode and the frequency ω_λ is a continuous function of l in the limit of a continuous leaking-mode ensemble.

We note that equation (6) contains no frequency δ-function in the infinite-depth limit and is formally identical with a non-conservative parametric transfer expression [HASSELMANN, 1968, eq. (3.4.9)].

The energy loss of the primary wave $\nu = (n, \boldsymbol{k}_n)$ due to trapped-trapped scattering gives rise to an energy gain of other modes $\lambda = (l, \boldsymbol{k}_l)$,

$$\frac{DF_\lambda}{Dt} = \frac{\partial F_\lambda}{\partial t} + \frac{\partial}{\partial x_j}(v_{\lambda j} F_\lambda) - \frac{\partial}{\partial k_j}\left(\frac{\partial\omega_\lambda}{\partial x_j} F_\lambda \right) = S_\lambda \tag{9}$$

where

$$S_\lambda = \omega_\lambda \frac{E_\nu}{\omega_\nu} \sum_{m \gtrless 0} T_{\lambda\nu\mu} F_\mu \delta(\omega_\nu + \omega_\mu - \omega_\lambda) \qquad (10)$$

with $\boldsymbol{k}_m = \boldsymbol{k}_l - \boldsymbol{k}_n$.

The second and third terms on the left side of equation (9) represent the change in the spectral density due to convection and refraction, respectively. (The refractive term enters only if the wave-guide is slowly varying in the mean, cf. [DORRESTEIN, 1960].

The source function (10) represents only the energy gained from the primary field $\nu = (n, \boldsymbol{k}_n)$. The complete transport equation for the scattered field includes further gain and loss terms due to scattering between modes ν, μ, λ within the spectral continuum (cf. section 4).

The energy gained by the leaking modes need not be considered. In the limit of an infinitely deep reflecting bottom, the ratio of local energy density (per unit volume) to total mode energy (per unit horizontal area) approaches zero for the deep (leaking) modes. Thus although the total energy gained by the leaking modes is finite, there is no observable change in local field quantities. Stated more simply in terms of the open, half-infinite model: the energy transferred to leaking modes is lost from the system by radiation to infinity.

The transfer integrals can be interpreted rather simply in terms of phonon collisions in a particle picture. The lowest-order transfer expressions (4)—(10) arise from collisions in which two phonons are annihilated and one is created (fig. 1). Energy and momentum of a phonon are proportional to frequency and wavenumber respectively The collision probability is proportional to the number densities $n = F/\omega$ of the ingoing phonons. Conservation of total energy and momentum in a collision is expressed by the frequency δ-function in equation (5) and the corresponding wavenumber side condition in equation (7). Modes with negative indices are represented by antiphonons with negative energy and momentum, the annihilation of an antiphonon corresponding to the creation of a phonon. To obtain the correct transfer expressions from the particle picture, only processes creating a single, positive-energy outgoing particle are allowed. Apart from this side condition, all collisions compatible with energy and momentum conservation are permissible*). In the present case, the relevant interactions involve an ingoing phonon ν of the primary acoustic field, an ingoing phonon μ or antiphonon $\bar{\mu}$ (fig. 1) of another trapped mode, and an outgoing phonon λ. The term phonon is used here in the wide sense to denote an arbitrary gravitational or acoustic mode).

*) The present particle picture [HASSELMANN, 1966] differs slightly from the more usual quantum-theoretical boson interpretation. In the boson picture, there are no antiparticles and no restrictions on the number of outgoing particles. However, the boson interaction rules are more complicated in the appropriate classical limit. In particular, the boson interpretation does not lead to a simple one-to-one correspondence between annihilated and created particles and individual terms in the transfer integrals.

Since the nonlinear coupling between two acoustic modes is normally very small, significant scattering occurs only if the mode μ (or $\bar{\mu}$) represents a surface gravity mode, internal gravity mode or a physical inhomogeneity (which can be treated formally as a mode of zero frequency [HASSELMANN, 1966]). In all of these cases, $\omega_\mu \ll \omega_\nu$, so that energy conservation yields $\omega_\lambda = \omega_\nu + \omega_\mu \approx \omega_\nu$. Momentum conservation implies that $\boldsymbol{k}_l \leq 0\,(\boldsymbol{k}_n)$, so that the outgoing phonon λ is again a high phase-velocity mode, and must therefore be either a trapped or leaking acoustic mode. Since λ is positive (as outgoing component), ν is also positive. However, the scattering component μ can be either a phonon or antiphonon (fig. 1).

The side conditions on the indices have been allowed for in equation (4)—(10). Equations (9), (10) describe only the energy gain of the outgoing acoustic component λ. The associated energy loss or gain of the low-frequency scattering field μ oder $\bar{\mu}$ is of the same form as (9), (10) but is generally small and can be neglected in the energy balance of the field μ (not considered here).

The above formalism applies to "weak" interactions satisfying the following criteria:

(i) The time scale τ of the energy transfer is large compared with a wave period. More precisely, τ must be large compared with the time interval or corresponding spatial interval required to resolve statistically the spectra occurring in the transfer

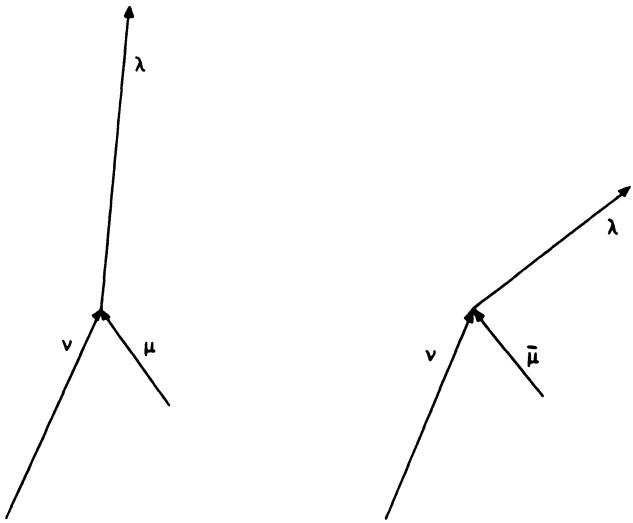

Fig. 1: Lowest order transfer diagrams for acoustic scattering. ν and λ represent acoustic phonons, μ and $\bar{\mu}$ the scattering phonon or antiphonon (surface wave, internal gravity wave, or waveguide inhomogeneity).

integrals (time and space resolution are related through the group velocity). The condition is normally satisfied for reasonable smooth scattering spectra; it implies essentially that the interactions are sufficiently weak that the linear concepts of normal modes, dispersion curves etc. retain their meaning.

(ii) The higher-order terms in the interaction expansion are small compared with the terms occurring in the lowest-order transfer expressions. For "well-behaved" statistical distributions, this condition follows from the first. However, exceptions can occur. For example, if the scattering field is highly intermittent, the higher statistical moments are exceptionally large, and the lowest-order scattering expressions, which depend only on the quadratic power spectra, may be a poor first approximation, although the computed transfer rates are weak. Alternatively, if the higher moments are "well behaved", but the spectra fall off very steeply at high wavenumbers, cubic and higher-order interactions which couple into the energetic part of the spectrum at low wavenumbers may dominate over the lowest-order quadratic interactions. In this case, the disparity in energy levels overrides the perturbation parameter of the nonlinear expansion.

The latter situation arises in the scattering of high-frequency acoustic modes in the cm—m range by surface gravity waves. The lowest-order (quadratic) transfer expressions represent the scattering due to short gravity waves with wavelengths comparable to the acoustic wavelength. However, the scattering can in fact be strongly modulated by the peak of the gravity-wave spectrum at wavelength of 10 m—500 m. The same effect occurs in the scattering of radar waves in the cm range at the ocean surface, cf. [WRIGHT, 1968, HASSELMANN and SCHIELER (to be published)]. The modulation can be treated rigorously only by a higher-order interaction analysis. For this reason the numerical results presented in sections 4 and 5 should be treated with caution for acoustic wavelengths shorter than 10 m.

After evaluating the transfer integrals, the primary and scattered fields are obtained by integrating the transport equations (4) and (9) under appropriate initial and boundary conditions. In the case of the primary field, the solution can be obtained immediately by integration along the wave-group trajectories, since there is no back-interaction from the scattered field*). Thus the problem reduces to the determination of the source function in equation (4). As example, we consider in the following section the damping factors γ_ν due to scattering by surface gravity waves.

The scattered field represents a more difficult radiative transfer problem, since the transport equation for all scattered modes are coupled. We return to this problem in section 4.

---

*) In general, second scattering leads to an energy transfer from the scattered field back to the original mode ν. However, the spectrum of the second-scattered field is continuous and yields only an infinitesimal contribution to the *line* E_ν.

3. Damping factors for scattering by surface waves

The general expressions for the coupling coefficients and transfer functions for acoustic-gravity-wave interactions are given in [ESSEN, 1970]. Numerical calculations

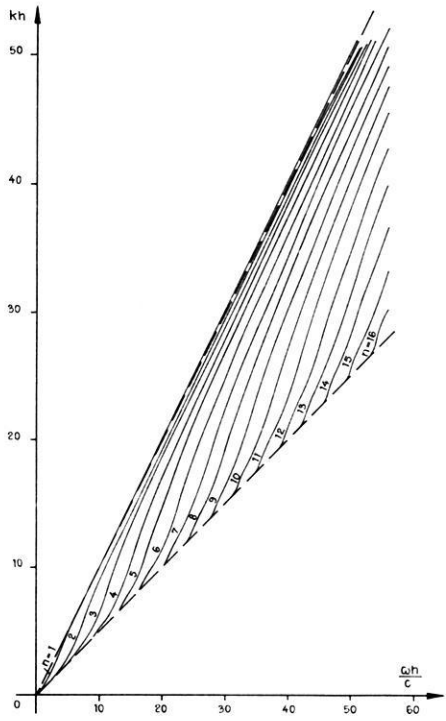

Fig. 2: Disperson curves for fluid/solid two-layer model. For better comparison with figs. 5 to 10 and 12 the axes have been interchanged with respect to the usual representation.

Sound velocity ratios:

Fluid : solid compressional : solid shear $= c : c_c : c_s = 1 : 2\sqrt{3} : 2$

Density ratio:

fluid : solid $= 1 : 2.5$

were carried out for the simplest model of a homogeneous fluid over a homogeneous elastic half space. The dispersion curves and physical parameters of this model are shown in fig. 2.

The gravity-wave field was represented by a PIERSON-MOSKOWITZ (1964) spectrum with a $\cos^4 \varphi$ spreading factor (fig. 3),

$$\left.\begin{aligned} G(\omega, \varphi) &= E_{PM}(\omega)\, S(\varphi) \\ E_{PM}(\omega) &= 0.0081\, g^2\, \omega^{-5}\, e^{-0.74\left(\frac{g}{\omega U}\right)^4} \\ S(\varphi) &= \begin{cases} \dfrac{8}{3\pi}\cos^4 \varphi, & 0 \le |\varphi| < \dfrac{\pi}{2} \\ 0, & \dfrac{\pi}{2} \le |\varphi| \le \pi \end{cases} \end{aligned}\right\} \quad (11)$$

where $G(\omega, \varphi)$ is the usual two-dimensional power spectrum of the surface elevation with respect to frequency $\omega = \sqrt{gk}$ and the wave direction φ relative to the mean wind U.

Equation (11) represents a one-dimensional family of self-similar spectra. We denote a particular member of the family by the nondimensional parameter $\beta = \hat{k}\, h$ where $\hat{k}$ is the gravity wavenumber corresponding to the peak frequency $\hat{\omega}$ of (11), $\hat{k} = \hat{\omega}^2/g$. The wind speed is related to β through

$$U = 0.877 \cdot \sqrt{\frac{gh}{\beta}}. \quad (12)$$

The spectrum (11) cuts off rapidly for wavenumbers less than $\hat{k}$ and approaches the wind-independent saturation form $G = 0.0081\, g^2 \omega^{-5} S(\varphi)$ for $k \gtrsim \hat{k}$ (more accurately, $k \gtrsim 2\hat{k}$).

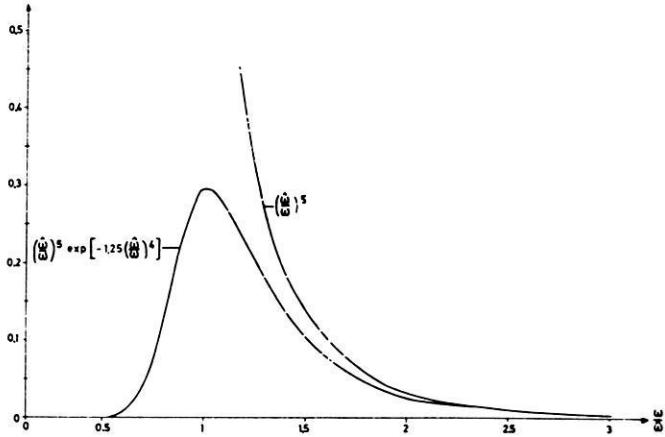

Fig. 3: PIERSON-MOSKOWITZ spectrum

$$E_{pm} = 0.0156 \cdot \frac{U^5}{g^3} \left(\frac{\hat{\omega}}{\omega}\right)^5 e^{-1.25\left(\frac{\hat{\omega}}{\omega}\right)^4}, \qquad \hat{\omega} = 0.877 \cdot \frac{g}{U}$$

Computed damping factors are presented in fig. 5, 7, 9 and 11. The horizontal damping factors γ_ν^{tt} have been decomposed into the individual contributions $\gamma_{\nu\lambda}^{tt}$ due to scattering into a particular trapped mode λ, so that

$$\gamma_\nu^{tt} = \sum_l \gamma_{\nu\lambda}^{tt} .$$

All damping factors are expressed in units of v_ν/h; thus the numerical coefficients $\tilde{\gamma}_\nu = \gamma_\nu h/v_\nu$ shown in the figures represent the damping rate in units of water depth h for a stationary spatially decaying mode,

$$E_\nu \sim e^{-\tilde{\gamma}_\nu \frac{x}{h}} .$$

In general, the damping factors are functions of β, the nondimensional frequency $\omega_\nu h/c$ (where c is the velocity of sound in water), the propagation direction α of the primary wave relative to the mean wind direction, and a fourth nondimensional parameter $\hat{\omega}/\omega_\nu$. The last parameter is so small that it can be neglected in calculating the coupling coefficients: the gravity-wave field may be regarded as frozen relative to the acoustic waves (this does not imply, however, that the Doppler shift of the scattered field is ignored, cf. section 4).

The overall dependence on the wind parameter β and propagation direction α can be deduced from kinematical relationships between the interacting wavenumbers, without going into details of the transfer functions. The wavenumbers occurring in the sum interaction $\nu + \mu \to \lambda$ are shown in fig. 4. For $|\omega_\mu/\omega_\nu| \ll 1$ the $\boldsymbol{k}_l$ loci are essentially circles. The difference interaction $\nu + \bar{\mu} \to \lambda$ yields the same gravity wavenumbers with opposite sign. The coupling coefficients for the sum and difference interaction are almost identical. Thus the difference interaction can be accounted for simply by superimposing a second gravity wave spectrum (11) with opposite propagation directions and considering then only sum interactions.

The largest and smallest wave numbers k_m for a given index combination n, l are

$$k_m^{\max} = k_l + k_n \quad \text{and} \quad k_m^{\min} = |k_l - k_n| .$$

If

$$k_m^{\max} h < \beta = \hat{k} h ,$$

all gravity wavenumbers occurring in the scattering process $\nu + \mu \to \lambda$ lie in the cut-off region of the Pierson-Moskowitz spectrum, and the damping rates are small. If

$$k_m^{\min} h \gtrsim \hat{k} h = \beta ,$$

the gravity wavenumbers all lie in the saturated range of the Pierson-Moskowitz spectrum, and the damping rate is equal to a saturation value which is independent of

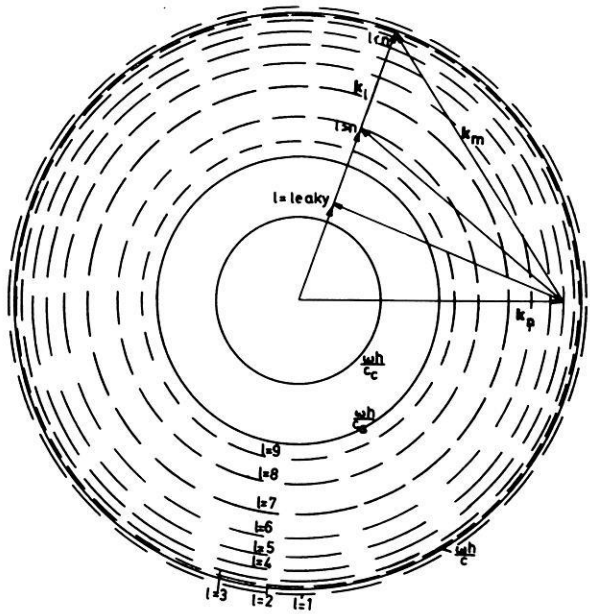

Fig. 4: Polar diagram of the primary acoustic mode k_n, scattering gravity-wave component k_m and scattered acoustic mode k_l for interaction.

$k_l = k_n + k_m$, $\omega_l = \omega_n + \omega_m \approx \omega_n = \omega$ for $\omega h/c = 30$ (constructed from fig. 1).

the wind speed. However, a directional dependence remains, the maximum damping generally occurring for propagation parallel or antiparallel to the mean gravity wave direction.

The values

$$\beta_{nl}^{\max} = k_m^{\max} h \text{ and } \beta_{nl}^{\min} = k_m^{\min} h$$

for a given interaction $\nu + \mu \to \lambda$ can be read off directly from the intercepts of the horizontal line $\omega_\lambda \approx \omega_\nu = \omega = \text{const}$ with the dispersion curves n and l in fig. 2.

Figs. 5, 7 and 9 show saturation damping factors for modes $n = 1$, 4 and 16 for propagation parallel or antiparallel to the wind ($\alpha = 0$ or π). The influence of the wind parameter β can be infered from the accompanying figures 6, 8 and 10, which show the curves

$$\beta_{nl}^{\max} \text{ and } \beta_{nl}^{\min}$$

for each interaction. A wind dependence exists only in the segments between

$$\beta_{nl}^{\min} \text{ and } \beta_{nl}^{\max}.$$

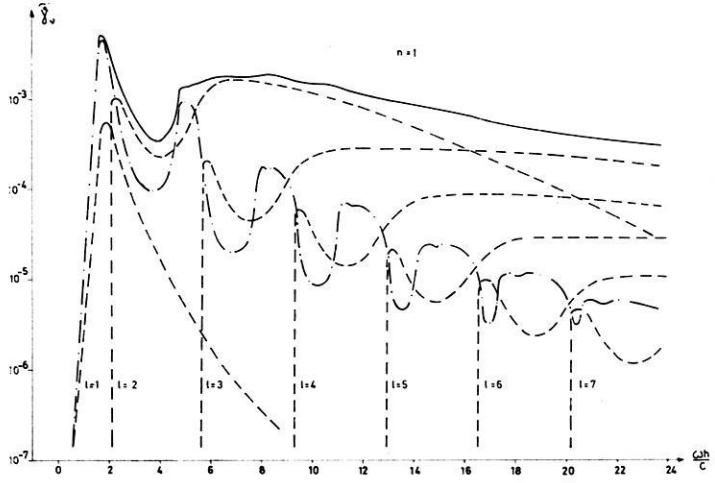

Fig. 5: Saturation damping factors $\tilde{\gamma}_\nu (\beta = 1)$, in units of inverse water depth for trapped-trapped and trapped-leaking interactions, wind parallel (or antiparallel) to the primary mode k_n, $n = 1$.

$\tilde{\gamma}^{tt}_{\nu\lambda}$ $\tilde{\gamma}^{tl}_{\nu}$ $\tilde{\gamma}_\nu = \sum_l \tilde{\gamma}^{tt}_{\nu\lambda} + \tilde{\gamma}^{tl}_{\nu}$

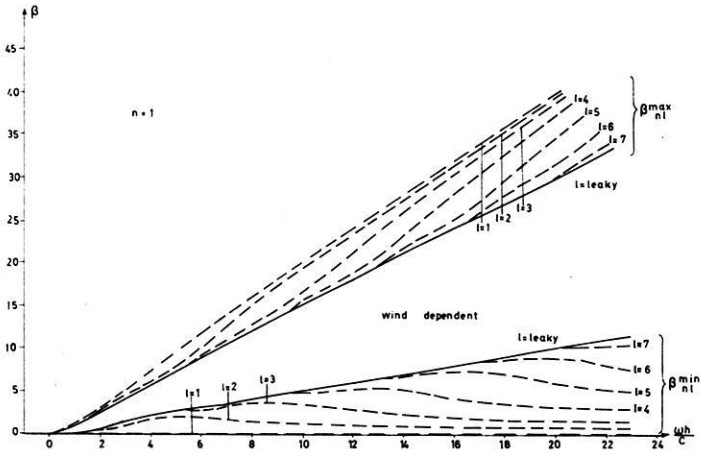

Fig. 6: Regions of wind dependence for trapped-trapped and trapped-leaking interactions, $n = 1$.

The attenuation is essentially zero for $\beta > \beta^{max}_{nl}$ and reaches an asymptotic saturated value for $\beta < \beta^{min}_{nl}$ (cf. fig. 5).

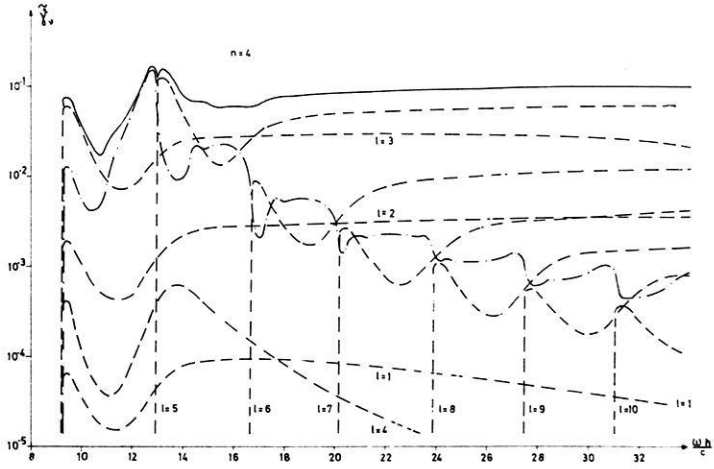

Fig. 7: Same as fig. 5, with $n = 4$.

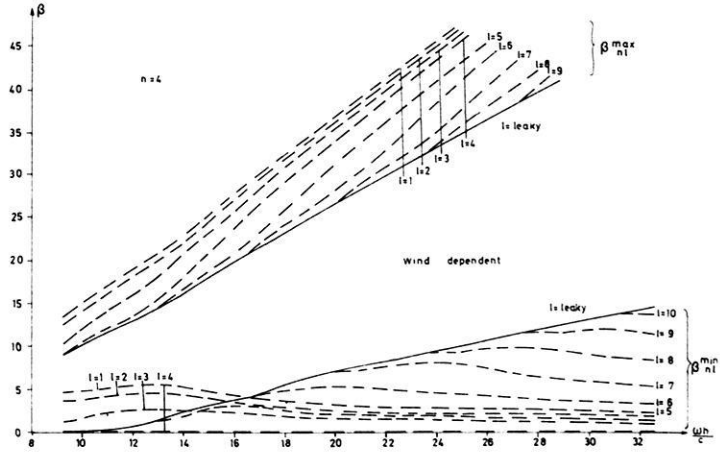

Fig. 8: Same as fig. 6, with $n = 4$ (cf. fig. 7).

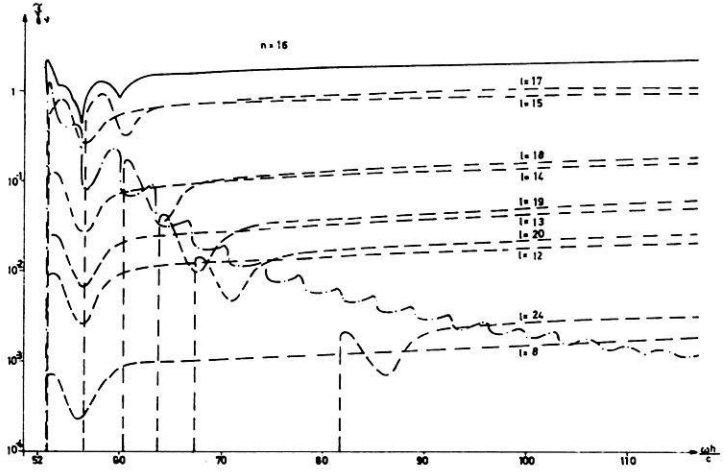

Fig. 9: Same as fig. 5, with $n = 16$.

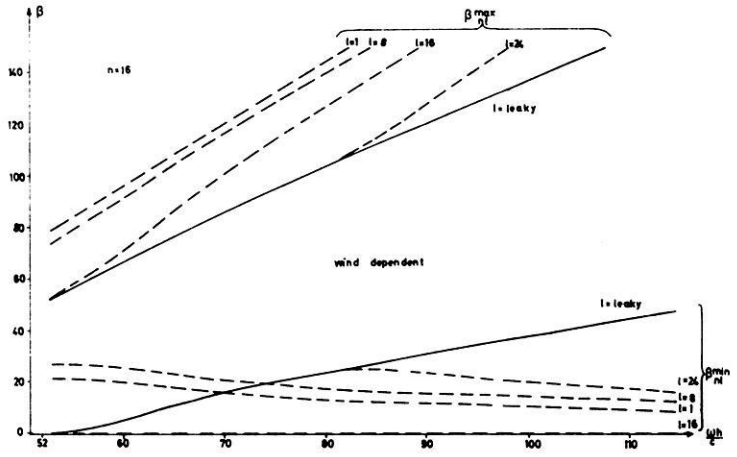

Fig. 10: Same as fig. 6, with $n = 16$ (cf. fig. 9).

For

$$\beta > \beta_{nl}^{\max},$$

the damping is negligible. For

$$\beta < \beta_{nl}^{\min} \text{ (or } \beta \lesssim {}^{\min}_{nl}/2),$$

the damping is essentially equal to the maximum saturation value. The same qualitative behaviour is found for propagation perpendicular to the wind, except that the transition range is smaller. The variation of the damping factors in the transition range is shown in fig. 11 for the case $n = 4$, $\omega_v h/c = 30$. In using figures 5—11 it should be noted that the Pierson-Moskowitz formula is applicable only to deep-water waves, $\beta \gtrsim 1$. For $\beta < 1$, the low-frequency end of the spectrum no longer increases appreciably with wind speed on account of the dissipative losses due to bottom frictions. As an order of magnitude estimate, we assume that for $\beta < 1$ the finite-depth spectrum levels off to the fully-developed form given by Pierson-Moskowitz for $\beta = 1$. Thus the region $\beta < 1$ in figures 6, 8 and 10 also correspond to wind-independent saturated regions. The saturation damping factors of figures 5, 7 and 9 have been computed for $\beta = 1$. The difference between the infinite-depth limit $\beta = 0$ and the finite-depth limit $\beta = 1$ is appreciable only in the regions

$$\beta_{nl}^{\min} < 1,$$

i.e. for low and very high frequencies and the case $l = n$ (cf. fig. 6, 8 and 10).

If β is greater than the largest value

$$\beta_n^{\max} = \sup_l (\beta_{nl}^{\max})$$

occurring in all interactions, the mode propagates virtually undamped. The corresponding wind velocity

$$U_n^{\text{pass}} = 0.877 \sqrt{g h / \beta_n^{\max}}$$

is shown in fig. 12 as a function of frequency. The curves for $n > l$ lie only slightly above U_1^{pass}. Thus to a good approximation it can be stated that *all modes propagate virtually undamped for wind velocities smaller than the "pass velocity"*

$$U^{\text{pass}} = U_1^{\text{pass}} = 0.877 \cdot \sqrt{\frac{gh}{2 k_1 h}} \approx 0.877 \sqrt{\frac{gh}{2 \frac{\omega h}{c}}}.$$

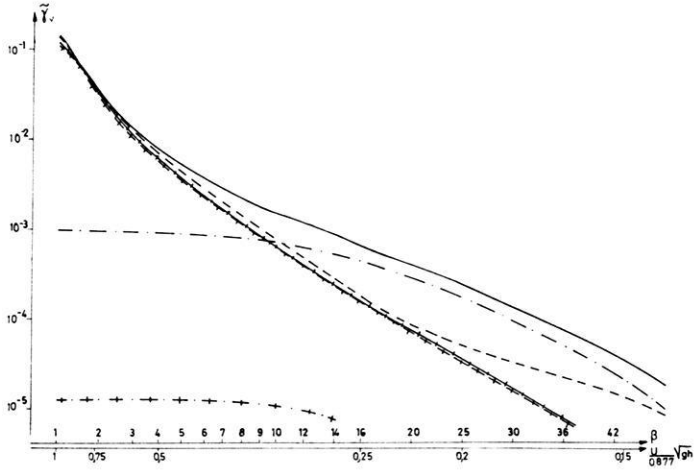

Fig. 11: Damping factors $\tilde{\gamma}_\nu$ in units of inverse water depth for trapped-trapped and trapped-leaking interactions in dependence of the wind parameter β for propagation parallel (or antiparallel) and perpendicular to the wind, $n = 4$, $\omega h/c = 30$.

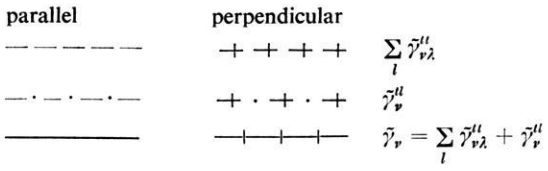

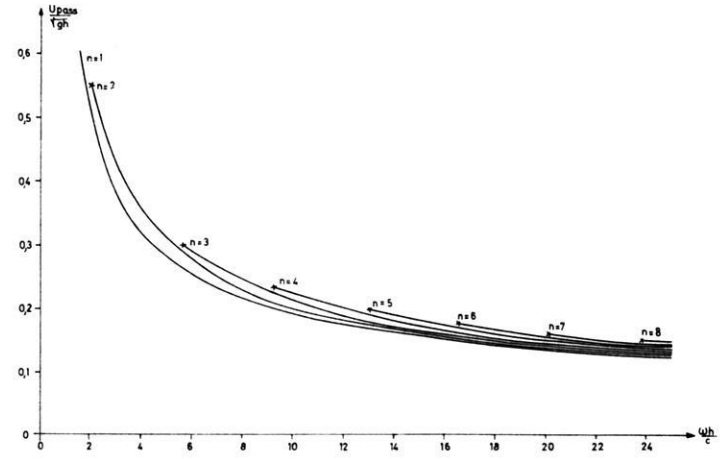

Fig. 12: Wind velocity U_n^{pass} as a function of frequency. For wind velocity less U_n^{pass} the mode n propagates nearly undamped.

Table 1: e-folding attenuation distances in meters.

	$h = 20$ m				$h = 50$ m			
$\omega/2\pi$ [Cps]	U [m/sec]	$n = 1$	$n = 4$	$n = 16$	U [m/sec]	$n = 1$	$n = 4$	$n = 16$
20	8.2 (U^{pass})	$7.0_{10}4$			6.8 (U^{pass})	$>_{10}7$		
	9.5	$1.9_{10}4$			11.0	$6.5_{10}5$		
	11.0	$7.2_{10}3$			15.0	$2.1_{10}5$		
	12.3 ($\beta = 1$)	$3.8_{10}3$			19.5 ($\beta = 1$)	$1.4_{10}5$		
100	3.0 (U^{pass})	$>_{10}7$			3.0 (U^{pass})	$>_{10}7$	$3.5_{10}6$	
	6.0	$1.4_{10}5$			8.0	$2.2_{10}6$	$1.0_{10}4$	
	9.0	$3.7_{10}4$			13.5	$3.9_{10}5$	$1.1_{10}3$	
	12.3 ($\beta = 1$)	$1.2_{10}4$			19.5 ($\beta = 1$)	$1.3_{10}5$	$4.8_{10}2$	
500	1.3 (U^{pass})	$>_{10}7$	$5.8_{10}6$		1.3 (U^{pass})	$>_{10}7$	$>_{10}7$	$4.5_{10}6$
	5.0	$9.2_{10}6$	$6.2_{10}3$		7.5	$>_{10}7$	$3.0_{10}4$	$6.6_{10}2$
	8.5	$1.7_{10}6$	$1.0_{10}3$		13.5	$>_{10}7$	$4.7_{10}3$	$5.1_{10}1$
	12.3 ($\beta = 1$)	$5.8_{10}5$	$2.0_{10}2$		19.5 ($\beta = 1$)	$>_{10}7$	$1.4_{10}3$	$3.1_{10}1$

	$h = 100$ m				$h = 500$ m			
$\omega/2\pi$ [Cps]	U [m/sec]	$n = 1$	$n = 4$	$n = 16$	U [m/sec]	$n = 1$	$n = 4$	$n = 16$
20	6,7 (U^{pass})	$>_{10}7$			6.7 (U^{pass})	$>_{10}7$	$>_{10}7$	
	13.5	$7.2_{10}5$			18.0	$>_{10}7$	$5.1_{10}4$	
	20.0	$1.9_{10}5$			30.0	$1.9_{10}6$	$5.4_{10}3$	
	27.5 ($\beta = 1$)	$5.9_{10}4$			43.5 ($\beta = 1$)	$6.6_{10}5$	$2.4_{10}3$	
100	3.0 (U^{pass})	$>_{10}7$	$>_{10}7$		3.0 (U^{pass})	$>_{10}7$	$>_{10}7$	$>_{10}7$
	11.0	$>_{10}7$	$3.1_{10}4$		16.5	$>_{10}7$	$1.5_{10}5$	$3.3_{10}3$
	19.0	$8.6_{10}6$	$5.1_{10}3$		30.0	$>_{10}7$	$2.3_{10}4$	$2.6_{10}2$
	27.5 ($\beta = 1$)	$2.9_{10}6$	$1.0_{10}3$		43.5 ($\beta = 1$)	$>_{10}7$	$7.2_{10}3$	$1.6_{10}2$
500	1.3 (U^{pass})	$>_{10}7$	$>_{10}7$	$>_{10}7$	1.3 (U^{pass})	$>_{10}7$	$>_{10}7$	$>_{10}7$
	10.0	$>_{10}7$	$\approx_{10}5$	$\approx_{10}3$	15.0	$>_{10}7$	$\approx 5_{10}5$	$\approx 2_{10}4$
	18.5	$>_{10}7$	$\approx_{10}4$	$\approx 3_{10}2$	29.0	$>_{10}7$	$\approx 7_{10}4$	$\approx 2_{10}3$
	27.5 ($\beta = 1$)	$>_{10}7$	$\approx 4_{10}3$	$\approx 5_{10}1$	43.5 ($\beta = 1$)	$>_{10}7$	$\approx 3_{10}4$	$\approx 4_{10}2$

Typical numerical values U^{pass} and e-folding decay distances for $U \geq U^{\text{pass}}$ are given in table 1. The corresponding attenuation distances for point-source fields consisting of a superposition of normal modes are given in ESSEN [1970].

For a given mode, the attenuation distance *increases* with increasing frequency. This is due partly to the fact that the trapped modes approach grazing incidence at large frequency: the number of ray reflections from the scattering surface for a given propagation distance becomes very small. Also, the fact that the wavenumber $k_n \to \infty$ as $\omega_\nu \to \infty$ implies that the area of the $\boldsymbol{k}_l$ wavenumber plane corresponding to interactions $\boldsymbol{k}_n + \boldsymbol{k}_m = \boldsymbol{k}_l$ with finite $k_m = 0\,(\hat{k})$ approaches zero for $\omega_\nu \to \infty$.

For a given frequency, the attenuation distance decreases with mode number. In the case of a point source located at a given depth in the wave guide, the proportion of energy in higher modes increases with frequency. Thus the frequency dependence of the net attenuation for a point source is given roughly by the diagonal in table 1. For intermediate distances, the modenumber dependence dominates: the half-value attenuation distance decreases with increasing frequency [ESSEN, 1970]. For large distances, the lowest modes dominate, so that the asymptotic differential decay distance increases with frequency.

4. The scattered field

In contrast to the primary wave field, the integration of the transport equations for the scattered field represents a complex radiative transfer problem. In general, the energy transferred between different scattered modes λ and λ' through processes $\lambda + \mu \to \lambda'$ is comparable with the energy gained from the primary mode ν through the process $\nu + \mu \to \lambda$. Thus all scattered modes are coupled, and the complete scattered field is described by an infinite set of nonlinear transport equations.

The solution is usually constructed iteratively, using single-, double- and higher-multiple scattering approximations. In the single-scattering approximation, only the scattering processes involving the primary mode are retained in the source function (equation (8)). Subsequent approximations are based on the full source functions, which are evaluated using the spectra determined from the previous iteration. The expansion is valid for distances not too far from the source, for which the scattered energy density is small compared with the energy density of the primary mode.

We consider in this section only the single-scattering approximation. The primary mode n is assumed to be generated by an isotropic, monochromatic point source of frequency ω_s at $\boldsymbol{x} = \boldsymbol{x}_s$ (fig. 13). The transport equation of the spectrum F_ν is then given by

$$v_{\nu i} \frac{\partial}{\partial x_i} F_\nu = \frac{Q_\nu}{2\pi k} \delta(\boldsymbol{x} - \boldsymbol{x}_s)\, \delta(k - k_n) - \gamma_\nu F_\nu \tag{13}$$

where Q_ν is the total energy input into the mode ν and $\boldsymbol{k}_n$ is the wavenumber of the mode ν corresponding to ω_s, $\omega_\nu\,(k_n) = \omega_s$.

The solution to (13) is

$$F_\nu(\boldsymbol{x}) = \frac{Q_\nu}{2\pi v_\nu \hat{r}} \delta(\boldsymbol{k} - \boldsymbol{k}_n) e^{-\frac{\gamma_\nu \hat{r}}{v_\nu}} \tag{14}$$

where

$$\hat{r} = |\boldsymbol{x} - \boldsymbol{x}_s|$$

$$\boldsymbol{k}_n = \frac{\boldsymbol{x} - \boldsymbol{x}_n}{\hat{r}} \cdot k_n$$

For a given primary field ν and scattering fields μ, the source term S_λ in the single-scattering equation (9) can be evaluated and the scattered field λ determined by integration along the wave-group trajectories,

$$F_\lambda = F_l(\boldsymbol{x}_r, \boldsymbol{k}_l) = \frac{1}{v_l} \int_{-\infty}^{0} S_\lambda(\boldsymbol{x}) \, \mathrm{d}s$$

where

$$\boldsymbol{x} = \boldsymbol{x}_r + \frac{\boldsymbol{k}_l}{k_l} s \tag{15}$$

Substituting expression (10) for S_λ and transforming to spectral densities $\tilde{F}(\omega, \varphi)$ with respect to frequency ω and propagation direction φ

$$\tilde{F}(\omega, \varphi) \, \mathrm{d}\omega \, \mathrm{d}\varphi = F(\boldsymbol{k}) \, \mathrm{d}\boldsymbol{k}, \quad \text{or} \quad \tilde{F}(\omega, \varphi) = \frac{k}{v} F(\boldsymbol{k})$$

equation (15) becomes

$$\tilde{F}_l(\omega_\lambda, \varphi_l) = \left\{ \frac{Q_\nu}{2\pi} T_{\lambda\nu\mu} \frac{\omega_\lambda}{{v_\lambda}^2 v_\nu k_\nu \omega_\nu \omega_\mu \sin^2 \Theta} \right.$$

$$\left. \tilde{F}_m(\omega_m, \varphi_m) e^{-\left(\frac{\gamma_\nu \hat{r}}{v_\nu} + \frac{\gamma_\lambda r}{v_\lambda}\right)} \right\}_{\text{resonance}} \tag{16}$$

where "resonance" refers to the particular position along the ray for which the resonant scattering conditions $\boldsymbol{k}_l = \boldsymbol{k}_n \pm \boldsymbol{k}_m$, $\omega_\lambda = \omega_\nu \pm \omega_\mu$ are satisfied. For fixed source and receiver positions $\boldsymbol{x}_s$, $\boldsymbol{x}_r$, and given frequency ω_λ and direction φ_l of the scattered mode, the resonance conditions can be satisfied at only one position $\boldsymbol{x}_{res}$ (fig. 13). The scattered energy is proportional to the scattering spectrum at $\boldsymbol{x}_{res}$ at the wavenumber $\boldsymbol{k}_m$. The resonance position $\boldsymbol{x}_{res}$ and wavenumber $\boldsymbol{k}_m$ can be constructed from the wavenumber scattering condition. noting that the moduli of the wavenumbers are determined by the frequencies. In principal, measurement of the two-dimensional scattered spectrum $\tilde{F}_l(\omega, \varphi)$ uniquely determines the two-dimensional spectrum $\tilde{F}_m(\omega, \varphi)$ of a homogeneous scattering field m.

The exponential factors in the solution (16) represent the scattering loss of the primary field (equation 14) along the path from x_s to x_{res} and the scattering loss of the field l along the path from x_{res} to x_r. Strictly, the energy loss due to trapped-trapped scattering should not be included in the single-scattering approximation. The corresponding exponential terms evolve automatically in the form of a TAYLOR series in successive, higher-scattering iterations. Accordingly, only the trapped-leaking inter-

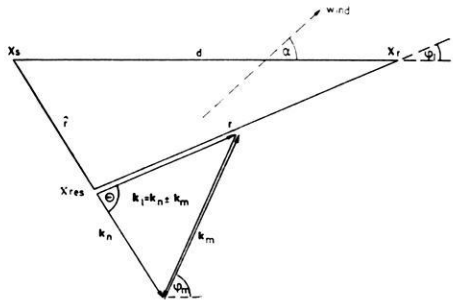

Fig. 13: Scattering path for interaction $\nu \pm \mu \rightarrow \lambda$. For given φ_l, k_l scattering occurs at only one resonance point x_{res}.

actions have been considered in the evaluation of the damping coefficients. In regions for which the single-scattering solution is a good approximation, the scattering losses are negligible. However, it is convenient to include the damping factors to remove singularities which would otherwise occur in the single-scattering solution (16) at $\Theta = 0$ and π (the single-scattering approximation is poor for $\Theta = 0$ and π).

As example, fig. 14 shows the computed total scattered energy per unit angle

$$F_l(\varphi_l) = \int_0^\infty \tilde{F}_l(\omega_\lambda, \varphi_l)\, \mathrm{d}\omega_\lambda$$

for the case of scattering by a surface-wave spectrum (11). The wave-guide model is the same as in the previous section. The wind parameter $\beta = 1$ corresponds to maximum scattering by a saturated surface wave spectrum. The source-receiver line was taken at an angle of 45° to the mean surface-wave direction to illustrate the directional asymmetry of the scattered field. Fig. 15 shows a similar asymmetry of the mean Doppler shift

$$\delta\omega_\mu(\varphi_l) = \frac{\int_0^\infty \tilde{F}_l(\omega_\lambda, \varphi_l)\, \omega_\mu\, \mathrm{d}\omega_\lambda}{\int_0^\infty \tilde{F}_l(\omega_\lambda, \varphi_l)\, \mathrm{d}\omega_\lambda}$$

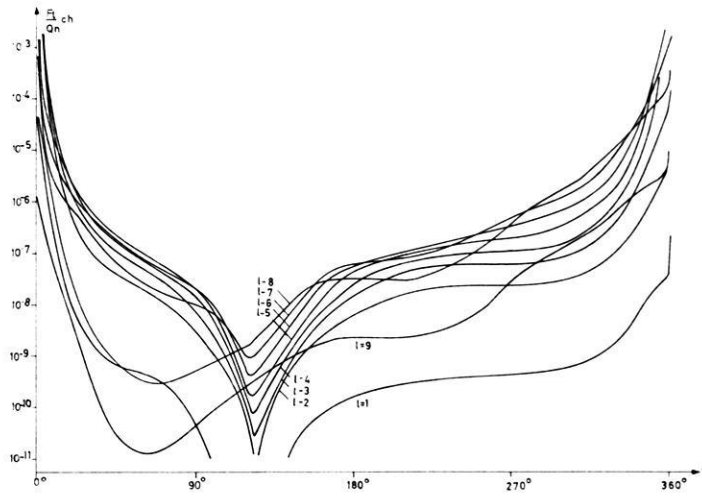

Fig. 14: Scattered energy of modes l from a primary mode $n = 4$, $\omega h/c = 30$.
The scattering surface wave spectrum is saturated, $\beta = 1$.
Source-receiver distance $d = 100 \cdot h$; mean surface-wave direction, $\alpha = 45°$.

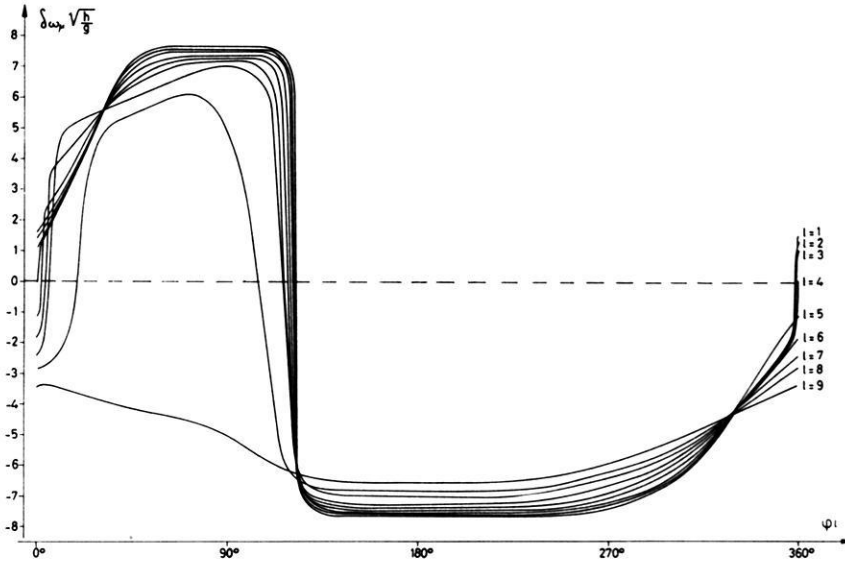

Fig. 15: Mean Doppler shift of the scattered energy per unit angle,
same parameters as in fig. 14.

Table 2: Total scattered energy densities of mode l.

l	E_l/E_n for $n = 4$, $\omega h/c = 30$					
	$\alpha = 0°$ $d/h = 5$	$\alpha = 0°$ $d/h = 20$	$\alpha = 0°$ $d/h = 100$	$\alpha = 0°$ $d/h = 500$	$\alpha = 45°$ $d/h = 100$	$\alpha = 90°$ $d/h = 100$
1	$1.1_{10}-4$	$4.5_{10}-4$	$2.3_{10}-3$	$1.5_{10}-2$	$1.2_{10}-3$	$4.3_{10}-4$
2	$1.2_{10}-2$	$4.7_{10}-2$	$2.4_{10}-1$	1.5	$1.2_{10}-1$	$4.3_{10}-2$
3	$1.1_{10}-1$	$4.3_{10}-1$	2.2	$1.3_{10}1$	1.0	$4.4_{10}-1$
4	$1.4_{10}-4$	$1.6_{10}-4$	$2.7_{10}-4$	$6.7_{10}-4$	1.1	4.6
5	$2.1_{10}-1$	$8.2_{10}-1$	3.9	$1.4_{10}1$	2.0	$7.7_{10}-1$
6	$3.3_{10}-2$	$1.3_{10}-1$	$5.3_{10}-1$	1.3	$3.7_{10}-1$	$1.5_{10}-1$
7	$1.0_{10}-2$	$3.6_{10}-2$	$1.1_{10}-1$	$1.5_{10}-1$	$1.1_{10}-1$	$4.7_{10}-2$
8	$3.5_{10}-3$	$9.0_{10}-3$	$1.3_{10}-2$	$1.8_{10}-2$	$2.6_{10}-2$	$1.3_{10}-2$
9	$1.4_{10}-4$	$2.9_{10}-4$	$3.9_{10}-4$	$7.7_{10}-4$	$7.2_{10}-4$	$2.5_{10}-4$

The total scattered energies $E_l = \iint \tilde{F}_l(\omega_\lambda, \varphi_l)\, d\omega_\lambda\, d\varphi_l$ for three angles $\alpha = 0°$, 45°, 90° between the source-receiver line and the mean wave direction are shown in table 2.

5. Conclusions

Scattering by surface gravity waves leads to a strong attenuation of acoustic modes. For fixed frequency, the attenuation increases with modenumber, for fixed modenumber, it decreases with increasing frequency.

All modes propagate virtually undamped for wind velocities smaller than a critical velocity U^{pass}. With increasing wind speed, the attenuation reaches a (frequency and mode-number dependent) maximum asymptotic value determined by the wind-independent ω^{-5} equilibrium gravity-wave spectrum.

In the case of a CW-source, the directional and frequency analysis of the scattered field yields information on the two-dimensional spectrum of the scattering field. Together with attenuation measurements, this provides an additional experimental check on the scattering theory. A similar analysis can be carried through in terms of the time delays for pulsed sinusoids, rather than the Doppler shifts of a CW-source.

The computed attenuation factors due to gravity-wave scattering are in order-of-magnitude agreement with measurements (e.g. [TOLSTOY and CLAY, 1966]). Observed Doppler shifts of the scattered field also suggest gravity-waves as a principal source of scattering [SCRIMGER, 1961, NICHOLS, 1967, URICK, 1968]. However, a quantitative comparison of theory with existing acoustic attenuation or scattering measurements is not possible on account of inadequate surface-wave information. Simultaneous measurements of the signal attenuation, the spectra of the surface waves and the scattered field characteristics are necessary to fully understand the observed attenuation processes.

References

DORRESTEIN, R.: Simplified method of determining refraction coefficients for sea waves, Journ. Geophys. Res., 65, 637–642, 1960.

ESSEN, H.-H.: Streuung niederfrequenter akustischer Eigenschwingungen im ozeanischen Wellenleiter. Berechnung der Übertragungsgrößen für Streuung an Oberflächenschwere wellen und Anwendung der Ergebnisse auf eine Punktquelle, wird veröffentlicht in den Hamburger Gophysikalischen Einzelschriften, 1970.

EWING, W. M., W. S. JARDETZKY, and F. PRESS: Elastic waves in layered media, McGraw-Hill, 1957.

FORTUIN, L.: A survey of literature on reflection and scattering of sound waves at the sea surface, Saclant ASW Research Centre, La Spezia (Italy) Technical Report No. 138, 1969.

HASSELMANN, K.: Feynman diagrams and interaction rules of wave-wave scattering processes, Rev. Geophys., 4, 1–32, 1966.

—: Nonlinear interactions treated by the methods of theoretical physics, Proc. Roy. Soc. A., 299, 77–100, 1967.

—: Weak-interaction theory of ocean waves, Basic Developments in Fluid Dynamics, 2, 117–182, 1968.

NICHOLS, R. H., and H. J. YOUNG, Fluctuations in low-frequency acoustic propagation in the ocean, Journ. Acoust. Soc. Am., 43, 716–722, 1967.

PEIERLS, R. E.: Zur kinetischen Theorie der Wärmeleitungen in Kristallen, Ann. d. Phys., 3, 1055–1101, 1929.

PIERSON, W. J., and L. MOSKOWITZ: A proposed spectral form for fully developed wind seas based on the similarity theory of S. A. Kitaigorodskii, Journ. Geophys. Res., 69, 5181 to 5190, 1964.

SCRIMGER, J. A.: Signal amplitude and phase fluctuations induced by surface waves in ducted sound propagation, Journ. Acoust. Soc. Am., 33, 239–247, 1961.

TOLSTOY, I., and C. S. CLAY: Ocean Acoustics, McGraw-Hill, 124–134, 1966.

URICK, R. J., G. R. LUND, and D. L. BRADLEY: Observations of fluctuation of transmitted sound in shallow water, Journ. Acoust. Soc. Am., 45, 683–690, 1969.

WRIGHT, J. W.: A new model for sea clutter, IEEE Trans. on Antennas and Propagation, AP-16, No. 2, 217–223, 1968.